Hindawi
Mathematical Problems in Engineering
Volume 2019, Article ID 8527183, 16 pages
https://doi.org/10.1155/2019/8527183

Research Article

Comparative Analysis between PI and Linear-ADRC Control of a Grid Connected Variable Speed Wind Energy Conversion System Based on a Squirrel Cage Induction Generator

Hammadi Laghridat,[1] **Ahmed Essadki**,[1] **and Tamou Nasser**[2]

[1]*High School of Technical Education (ENSET), Mohammed V University, Rabat, Morocco*
[2]*National High School for Computer Science and Systems (ENSIAS), Mohammed V University, Rabat, Morocco*

Correspondence should be addressed to Hammadi Laghridat; hammadi.laghridat@um5s.net.ma

Received 10 December 2018; Revised 21 January 2019; Accepted 3 March 2019; Published 26 March 2019

Academic Editor: Denizar Cruz Martins

This paper aims at contributing to the modeling and control of a variable speed Wind Energy Conversion System (WEC-System) based on a Squirrel Cage Induction Generator (SCI-Generator). The connection between the SCI-Generator and the main utility grid is achieved by back-to-back three phase power converters (Generator and Grid Side Converters). A new control strategy named the Active Disturbance Rejection Control (ADRC) is proposed and utilized to control the Wind Energy Conversion (WEC) system based on the SCI-Generator. The objective is to control both the generator and the grid side converters in order to operate the system and to ensure the connection with the power grid. The first converter is used to control the SCI-Generator speed and field to extract the available maximum power from the wind turbine by using a Maximum Power Point Tracking (MPPT) technique and, also, to ensure that the extracted power does not exceed its rated value in case of strong wind speeds; in this case a pitch actuator system is used to control the blades pitch angle of the wind turbine. The second converter is used to control the active and reactive powers injected into the utility grid as well as to regulate the DC-Link Voltage. This control takes into account the rejection of internal disturbances as the variation of electrical parameters (the resistance, the inductance…) and the external disturbances as voltage dips and frequency droops in the main grid. To test and validate the performances of the proposed controller, a series of simulations were developed under MATLAB/Simulink environment, and the results have demonstrated the effectiveness of the proposed control under different case of simulations.

1. Introduction

Very early in the history of technology, wind was exploited to extract mechanical energy from it, where the conversion of wind energy into mechanical energy is indeed relatively easy; it is only necessary to have a satisfactory potential and to resist the whims of excessive winds. Commonly, mechanical devices called "wind turbines" are utilized in this purpose. And for the conversion of this power into electrical energy, electrical generators are used. Generally, there are three types of generators: Doubly Fed Induction Generators (DFIG), Squirrel Cage Induction Generators (SCIG), and Permanent Magnet Synchronous Generators (PMSG). For the high-power production, the SCI-Generators are the one to be used; their main interest lies in their simple structure where the connection with the utility grid is accomplished by back-to-back power converters.

The proliferation of wind turbines has led electrical engineering researchers to conduct investigations to improve the efficiency of electromechanical conversion and the quality of the energy supplied. For better operation of these systems, Maximum Power Point Tracking (MPPT) algorithms are

needed to improve the energy efficiency and to extract the maximum power available from the wind turbine. In literature, several techniques were used going from the utilization of classical extreme algorithms such as Perturb and Observes (P&O), Incremental Conductance (INC), and Hil Climbing (HCS) [1] to those based on artificial intelligence as Fuzzy Logic and Neural networks [2]. However, the wind turbine has an advantages that it can be reliably characterized by its specific function $C_p(\lambda)$. This is why the literature commonly refers to MPPT algorithms that seek to bring the operating point to the maximum point that this function forms; we can find among them the tip speed ratio (TSR) and Optimal Torque Control (OTC) techniques; the last one is to be used in this paper.

To ensure the accurate integration of the WEC-System with the utility grid, the regulation of active and reactive powers is needed as well as the synchronization of voltage and frequency. In this context numerous publications are found in literature as, in [3], the authors proposed an indirect vector control of a Squirrel Cage Induction Generator wind turbine where the objective is to control the DC-bus voltage and the reactive power by using the classical Proportional Integrator (PI) controller, authors in [4] used the Sliding Mode Control to drive the WEC-System based on a SCI-Generator, authors in [5] proposed a Fuzzy Logic Control of a variable speed cage machine wind generation system, and, in [6], the authors have used the Backstepping technique, Furthermore, additional types of controllers were also considered for squirrel cage-based WEC-Systems as cited in [3–16]. Nevertheless, another controller appeared in the last 10 years and it is used for the control applications in several area; this controller is known as the Active Disturbance Rejection Controller (ADRC); it is proposed by Jingqing Han [10]. However, to the authors' best knowledge, very few publications are available in the literature that address the issue of controlling Wind Energy Conversion systems, where in [11] the authors proposed the control of a wind system based on a DFIG by the ADRC technique and in [12] the authors discussed the control of a direct driven wind turbine based on Permanent Magnetic Synchronous Generator by ADRC, but for the WEC SCI-Generator the application of this control cannot be found. The main advantage of this controller lies in the real time rejection of internal and external disturbances based on an extended state observer (ESO). There are different types of disturbances, whether internal disturbances as variation of the generator parameters (resistance or inductance) and external disturbances like the instability of the grid caused either by voltage droops or frequency variation. As a result, we propose in this paper the application of Linear-ADRC controller to Wind Energy Conversion System based on SCI-Generator.

The contribution of this work lies in the development of a Linear Active Disturbance Rejection controller (Linear-ADRC) to control both the generator and the grid side converters. The first control is used to regulate the mechanical speed of the generator in order to guarantee the extraction of maximum power available from the wind at different speeds; also another attention is given to the pitch angle control in order to operate the wind turbine in high wind speed and to limit the extracted power (The generator side converter). The second control is used to regulate the DC-Link Voltage as well as the active reactive powers exchange with the grid (the grid side converter). To summarize, this paper seeks to evaluate the dynamical performances and sensitivity to SCIG parameter changes with comparing the classical Indirect Field Oriented Control based on the PI controller and the new Linear Active Disturbance Rejection Control.

This paper is organized as follows, where Section 2 presents the modeling of the Wind Energy Conversion System based SCI-Generator. The Optimal Torque Control and pitch angle control are given in Section 3. The Wind Energy Conversion System control by PI controller is detailed in Section 4, the application of the Linear Active Disturbance Rejection Control of the Wind Energy Conversion System is demonstrated in Section 5, and, finally, the simulation results and discussions are presented in Section 6.

2. Wind Energy Conversion (WEC) System Model

This section deals with the Wind Energy Conversion (WEC) system model. The configuration of the SCI-Generator and it's illustrated in Figure 1. It consists of two parts. The first part consists with the turbine model, the SCI-Generator, and the AC/DC converter (The stator side). The second part of the model consists of the DC-Link, the DC/AC converter, and a filter (The grid side).

The aim of the wind turbine is to capture the wind kinetic energy and convert it to a torque that rotates the rotors blades. Thereafter, the SCI-Generator converts the mechanical power (P_m) into an electrical power to be exchanged with the grid through the power converters (AC/DC/AC). Firstly, we began with the modeling the mechanical part and then the electrical part.

2.1. Turbine Model (Mechanical Part). The mechanical power available from the mind turbine rotor is given by the following:

$$P_m = \frac{1}{2} C_p(\lambda, \beta)\, \rho A w^3 \tag{1}$$

where C_p is the aerodynamic coefficient; β is the blades pitch angle, λ is the turbine tip speed ratio, and A is the turbine blades area. ρ and w are representing the air density and the wind speed, respectively.

The tip speed ratio is given by

$$\lambda = \frac{R\Omega_{tur}}{v} \tag{2}$$

where Ω_{tur} is the turbine speed and R is the turbine radius blades.

The mechanical torque T_m is given by

$$T_m = \frac{P_m}{\Omega_{tur}} \tag{3}$$

The coefficient C_p is a nonlinear equation which depends on the tip speed λ, and it is expressed by

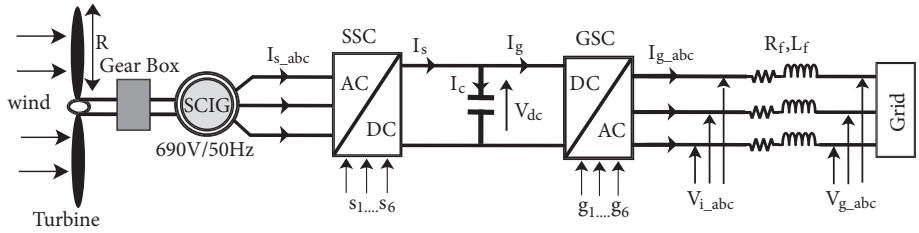

Figure 1: Structure of a Wind Energy Conversion (WEC) System Using SCI-Generator.

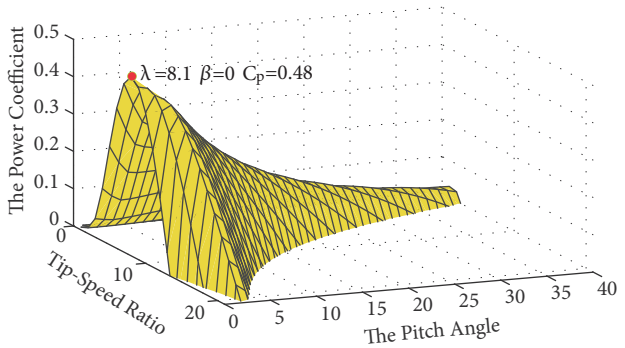

Figure 2: The Aerodynamic coefficient for WEC-System.

$$C_p(\lambda,\beta) = c_1\left(c_2\frac{1}{\lambda^i} - c_3\beta - c_4\right)exp^{(-c_5/\lambda^i)} + c_6\lambda \quad (4)$$

where

$$\frac{1}{\lambda^i} = \frac{1}{\lambda + c_7\beta} - \frac{c_8}{\beta^3 + 1} \quad (5)$$

where $c_1 = 0.5176$, $c_2 = 166$, $c_3 = 0.4$, $c_4 = 5$, $c_5 = 21$, $c_6 = 0.0068$, $c_7 = 0.08$, and $c_8 = 0.035$.

Figure 2 represents C_p according to λ for different values of pitch angle β. The figure shows that C_p is maximum when $\beta = 0deg$ and $\lambda = 8.1$.

The gearbox is a device which adapts the (slow) turbine speed Ω_{tur} to the (fast) generator speed Ω_{mec}. This gearbox can be mathematically modeled by the following:

$$T_g = \frac{T_m}{G} \quad (6)$$

$$\Omega_{tur} = \frac{\Omega_{mec}}{G} \quad (7)$$

where G is the gearbox ratio.

The system mechanical equation is given by

$$J\frac{d\Omega_{mec}}{dt} = T_m - T_{em} - f\Omega_{mec} \quad (8)$$

where T_{em} is the induction generator electromagnetic torque and f is the friction coefficient. J represents the total inertia of the generator (J_{SCIG}) and the turbine (J_{tur}) which can be calculated by

$$J = \frac{J_{tur}}{G^2} + J_{SCIG} \quad (9)$$

2.2. SCI-Generator Model. The Squirrel Cage Induction (SCI) generator dynamic model in the direct-quadrature frame is presented by

$$\frac{d\Psi_{sd}}{dt} = -R_s i_{sd} + \omega_s \Psi_{sq} + v_{sd} \quad (10)$$

$$\frac{d\Psi_{sq}}{dt} = -R_s i_{sq} - \omega_s \Psi_{sd} + v_{sq} \quad (11)$$

$$\frac{d\Psi_{rd}}{dt} = -R_r i_{rd} + \omega_r \Psi_{rq} \quad (12)$$

$$\frac{d\Psi_{rq}}{dt} = -R_r i_{rq} - \omega_r \Psi_{rd} \quad (13)$$

where i_{sd} and i_{sq} are the direct and quadrature stator currents; i_{rd} and i_{rq} are the direct and quadrature rotor currents. Ψ_{sd} and Ψ_{sq} are the direct-quadrature frame stator fields; Ψ_{rd} and Ψ_{rq} are the direct-quadrature frame rotor fields. The stator voltages in the direct-quadrature frame are v_{sd} and v_{sq}. Also, R_s and R_r are the stator and the rotor phases resistances; and ω_r is the rotor electrical speed and ω_s is the stator electrical speed.

The stator and rotor fields equations are given by

$$\Psi_{sd} = L_s i_{sd} + M i_{rd} \quad (14)$$

$$\Psi_{sq} = L_s i_{sq} + M i_{rq} \quad (15)$$

$$\Psi_{rd} = L_r i_{rd} + M i_{sd} \quad (16)$$

$$\Psi_{rq} = L_r i_{rq} + M i_{sq} \quad (17)$$

where M is the mutual inductance and L_s and L_r are the stator inductance and the rotor inductance respectively.

The electromagnetic torque T_{em} is expressed by

$$T_{em} = \frac{pM}{L_r}\left(\Psi_{rd} i_{sq} - \Psi_{rq} i_{sd}\right) \quad (18)$$

where p is the pole pairs number.

The active and reactive powers (P_s, Q_s) produced by the SCI-Generator can be written as follows:

$$P_s = \frac{3}{2}\left(v_{sd} i_{sd} + v_{sq} i_{sq}\right) \quad (19)$$

$$Q_s = \frac{3}{2}\left(v_{sq} i_{sd} - v_{sd} i_{sq}\right) \quad (20)$$

The state model of the SCI-Generator can be written as follows:

$$\frac{di_{sd}}{dt} = -k_1 i_{sd} + \omega_s i_{sq} + k_2 \Psi_{rd} + k_3 \Omega_{mec} \Psi_{rq} + k_4 v_{sd} \quad (21)$$

$$\frac{di_{sq}}{dt} = -k_1 i_{sq} - \omega_s i_{sd} + k_2 \Psi_{rq} - k_3 \Omega_{mec} \Psi_{rd} + k_4 v_{sq} \quad (22)$$

$$\frac{d\Psi_{rd}}{dt} = k_5 i_{sd} - k_6 \Psi_{rd} + (\omega_s - p\Omega_{mec}) \Psi_{rq} \quad (23)$$

$$\frac{d\Psi_{rq}}{dt} = k_5 i_{sq} - k_6 \Psi_{rq} - (\omega_s - p\Omega_{mec}) \Psi_{rd} \quad (24)$$

where

$$\begin{aligned} k_1 &= \frac{L_r^2 R_s + M^2 R_r}{\sigma L_s L_r^2}; \\ k_2 &= \frac{R_r M}{\sigma L_s L_r^2}; \\ k_3 &= \frac{p R_r}{\sigma L_s L_r}; \\ k_4 &= \frac{1}{\sigma L_s}; \\ k_5 &= \frac{M R_r}{L_r}; \\ k_6 &= \frac{R_r}{L_r}. \end{aligned} \quad (25)$$

with $\sigma = (1 - M^2/L_s L_r)$ being the dispersion coefficient.

2.3. Grid Side Converter (GSC) Model. The grid side equations can be expressed by

$$\begin{aligned} V_{ga} &= R_f i_{ga} + L_f \frac{di_{ga}}{dt} + v_{ia} \\ V_{gb} &= R_f i_{gb} + L_f \frac{di_{gb}}{dt} + v_{ib} \\ V_{gc} &= R_f i_{gc} + L_f \frac{di_{gc}}{dt} + v_{ic} \end{aligned} \quad (26)$$

Applying the d-q transformation, (26) become as follows:

$$v_{id} = R_f i_{gd} + L_f \frac{di_{gd}}{dt} - \omega_g L_f i_{iq} + v_{gd} \quad (27)$$

$$v_{iq} = R_f i_{gq} + L_f \frac{di_{gq}}{dt} + \omega_g L_f i_{id} + v_{gq} \quad (28)$$

where v_{gd} and v_{gq} are the grid voltage components (direct and quadrature) and i_{gd} and i_{gq} are the grid current components (direct and quadrature). The voltages v_{id} and v_{iq} are the source inverter direct and quadrature components; R_f and L_f are the resistance and the inductance of the filter. $\omega_g = 2\pi f_g$; f_g is the grid frequency, it is given by the PLL (Phase Locked Loop).

The above equations can be written as

$$\frac{di_{gd}}{dt} = -k_7 i_{gd} + \omega_g i_{gq} + k_8 (v_{id} - v_{gd}) \quad (29)$$

$$\frac{di_{gq}}{dt} = -k_7 i_{gq} - \omega_g i_{gd} + k_8 (v_{iq} - v_{gq}) \quad (30)$$

where $k_7 = R_f/L_f$ and $k_8 = 1/L_f$.

The active and reactive powers (P_g, Q_g) injected to grid are given by the following:

$$P_g = \frac{3}{2} (v_{gd} i_{gd} + v_{gq} i_{gq}) \quad (31)$$

$$Q_g = \frac{3}{2} (v_{gq} i_{gd} - v_{gd} i_{gq}) \quad (32)$$

The voltage equation of the DC-Link can be written as

$$C \frac{dv_{dc}}{dt} = i_{dc} = i_s - i_g \quad (33)$$

where v_{dc} and i_{dc} are the DC-Link Voltage and the DC-Link current. The currents i_s and i_g are the SCI-Generator side current and the grid side current, respectively, and C is the DC-Link Capacitor.

3. Optimal Torque Control and Pitch Angle Control

3.1. Optimal Torque Control (MPPT Technique). The Maximum Power Point Tracking is a technique used to extract the maximum power from the turbine for different wind speed. It is necessary that the turbine speed must be adjusted relatively to the wind speed to obtain the maximum available power from the turbine. Therefore, the tip speed ratio must be maintained to an optimum value of the tip speed ratio $(\lambda = \lambda^{opt})$ and of the power coefficient $(C_p = C_p^{max})$.

The maximum mechanical power can be expressed as a function of the rotational speed:

$$P_m^{max} = \frac{1}{2} \rho \pi R^5 \frac{C_p^{max}}{\lambda^{opt^3}} \frac{\Omega_{mec}^3}{G^3} \quad (34)$$

The optimal torque (desired torque) is such that

$$T_{em}^{ref} = C_{opt} {\Omega_{mec}}^2 \quad (35)$$

where the Optimal Torque Coefficient is

$$C_{opt} = \frac{1}{2} \rho \pi R^5 \frac{C_p^{max}}{\lambda^{opt^3}} \frac{1}{G^3} \quad (36)$$

The mechanical speed reference is given by

$$\Omega_{mec}^{ref} = \frac{G \lambda^{opt}}{R} w \quad (37)$$

3.2. Pitch Angle Control. In the previous part, it has been shown that the maximum power is generated by MPPT Technique. Nevertheless, it is necessary to limit the power of the WEC-System; As a pitch angle control is used it is operated by acting on the orientation of the turbine blades area β, to avoid the power not exceeding its rated value in case of strong wind speeds.

The equation between the power P and the pitch angle β is approached by a first-order system, and this approach allows controlling the SCI-Generator power by a closed loop PI controller [3].

The equation between β and β^{ref} can be written under the following form (closed loop):

$$\beta = \frac{1}{1 + T_\beta s}\beta^{ref} \tag{38}$$

where s is a Laplace operator; T_β is the time constant of the pitch servo. The pitch angle control scheme is depicted in the Figure 3.

The PI controller is used to decrease the error signal between the rated power and the measured power. It is to produce at its output the reference pitch angle β_{ref}. In normal case, the pitch angle rates are at the maximum and minimum ($\dot{\beta}_{min}, \dot{\beta}_{max}$) allowable values between ±10 *degrees/s* and the angle (β_{min}, β_{max}) allowable between (0 *degrees*, 45 *degrees*).

4. Wind Energy Conversion System Control by PI

This section focuses on the strategy adopted to control the WEC-System using a SCI-Generator by PI Controller. Two controllers are used. The first is used to control the stator side converter, where the objective is to extract maximum power form the wind turbines (regulates the electromagnetic torque and the field of the SCI-Generator). The second controller (grid side converter control) is used to regulate the DC-bus voltage and to control the grid powers (active and reactive), which is depicted in Figure 4.

4.1. Stator Side Converter (SSC) Control by PI. The PI controller is considered as the most used to control the WEC-System based on a SCI-Generator, because of its simplest implementation. The objective in this part is to regulate the electromagnetic torque and the field of the SCI-Generator to extract the maximum mechanical power P_m available from the turbine for different wind speeds.

To archive the decoupled control of electromagnetic torque and field of the generator, the Indirect Rotor Field Oriented Control (IRFOC) used let

$$\begin{aligned} \Psi_{rq} &= 0; \\ \Psi_{rd} &= \Psi_r \end{aligned} \tag{39}$$

Then the SCI-Generator Model

$$\frac{di_{sd}}{dt} = -k_1 i_{sd} + \omega_s i_{sq} + k_2 \Psi_{rd} + k_4 v_{sd} \tag{40}$$

$$\frac{di_{sq}}{dt} = -k_1 i_{sq} - \omega_s i_{sd} - k_3 \Omega_{mec} \Psi_{rd} + k_4 v_{sq} \tag{41}$$

$$\frac{d\Psi_{rd}}{dt} = k_5 i_{sd} - k_6 \Psi_{rd} \tag{42}$$

The electromagnetic torque equation is given by

$$T_{em} = \frac{pM}{L_r}\Psi_{rd} i_{sq} \tag{43}$$

The electromagnetic torque expression is a proportion with the quadrature stator current provided that the direct rotor field is constant, for this we will regulate field of the rotor.

From (42) and (43), the reference quadrature stator current and the estimated direct component of the rotor field are given by

$$i_{sq}^{ref} = \frac{L_r}{pM\Psi_{rd}^{ref}} T_{em}^{ref} \tag{44}$$

$$\Psi_{rd}^{est} = \frac{k_5}{k_6 + s} i_{sd} \tag{45}$$

where s is a Laplace operator and the torque T_{em}^{ref} is the optimal torque (generated by MPPT).

The rotor field angle is

$$\theta_f = \int (\omega_{sl} + p\Omega_{mec})\, dt \tag{46}$$

with the slip frequency being obtained by

$$\omega_{sl} = \frac{R_r M}{L_s} \frac{i_{sq}}{\Psi_{rd}^{est}} \tag{47}$$

The compensation and the coupling terms are gathers in the following:

$$e_{sd} = \frac{1}{k_4}\omega_s i_{sq} + \frac{k_2}{k_4}\Psi_{rd} \tag{48}$$

$$e_{sq} = \frac{1}{k_4}\omega_s i_{sd} + \frac{k_3}{k_4}\omega_{mec}\Psi_{rd} \tag{49}$$

Figure 5 depicts the control of stator side converter scheme of the SCI-Generator by PI Controller.

4.2. Grid Side Converter (GSC) Control by PI. The grid side converter is used to deliver the generated power into the electrical grid; the first controller is used to regulate the DC-Link Voltage and the other controller to control the power injected into the grid during wind variations to achieve a unit power factor. Therefore for independent control of the grid active and the grid reactive power, we use Voltage Oriented (VOC) Control. Hence $v_{gd} = 0$ and $v_{gq} = v_g$, and therefore the output P_g and Q_g of the WEC-System can be written as

$$P_g = \frac{3}{2} v_g i_{gq} \tag{50}$$

$$Q_g = \frac{3}{2} v_g i_{gd} \tag{51}$$

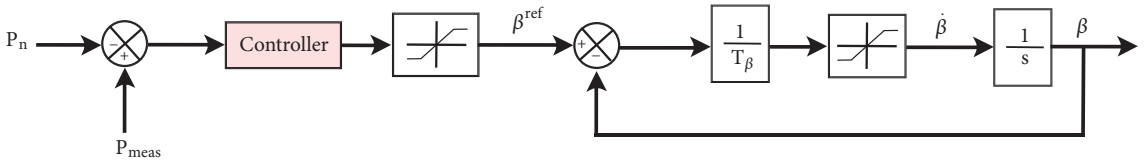

Figure 3: Pitch Angle Control.

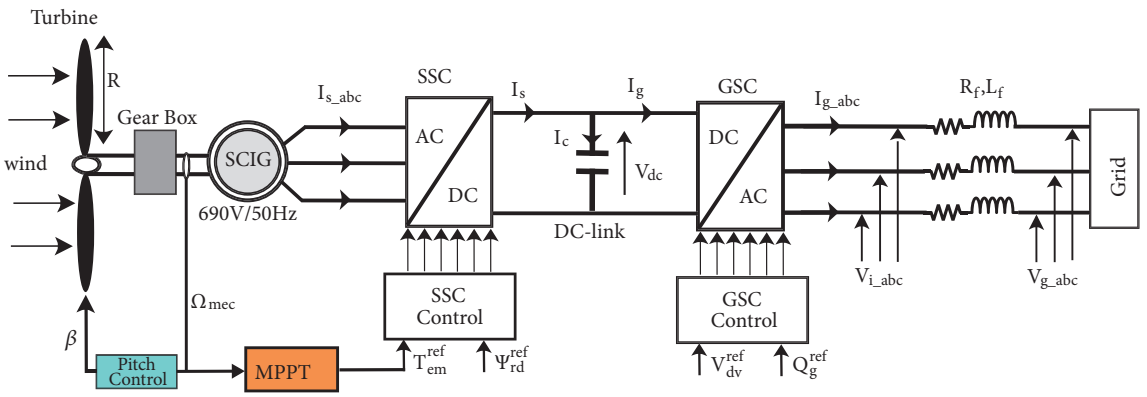

Figure 4: Control Wind Energy Conversion (WEC) System Using SCI-Generator.

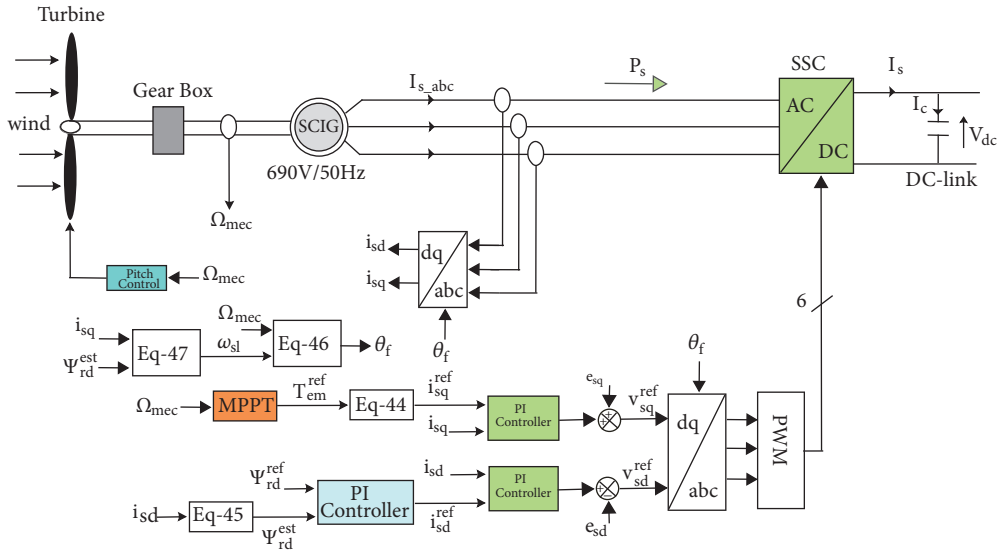

Figure 5: The Generator Side Converter Control by PI.

And the grid currents

$$\frac{di_{gd}}{dt} = -k_7 i_{gd} + \omega_g i_{gq} + k_8 v_{id} \tag{52}$$

$$\frac{di_{gq}}{dt} = -k_7 i_{gq} - \omega_g i_{gd} + k_8 \left(v_{iq} - v_g\right) \tag{53}$$

From (51) the reference current i_{gd}^{ref} is calculated by the desired delivery of reactive power:

$$i_{gd}^{ref} = \frac{2}{3v_g} Q_g^{ref} \tag{54}$$

The compensation and the coupling terms are expressed in the following:

$$e_{gd} = v_{gd} - \frac{1}{k_8}\omega_g i_{gq} \tag{55}$$

$$e_{gq} = v_{gq} + \frac{1}{k_8}\omega_g i_{gd} \tag{56}$$

where $v_{gd} = 0$ and $v_{gq} = v_g$. Figure 6 depicts the control of grid side converter scheme of the SCI-Generator by PI Controller.

4.3. The Synthesis of PI Correctors. To tune the parameters of the PI controllers (the proportional gain controller K_p and

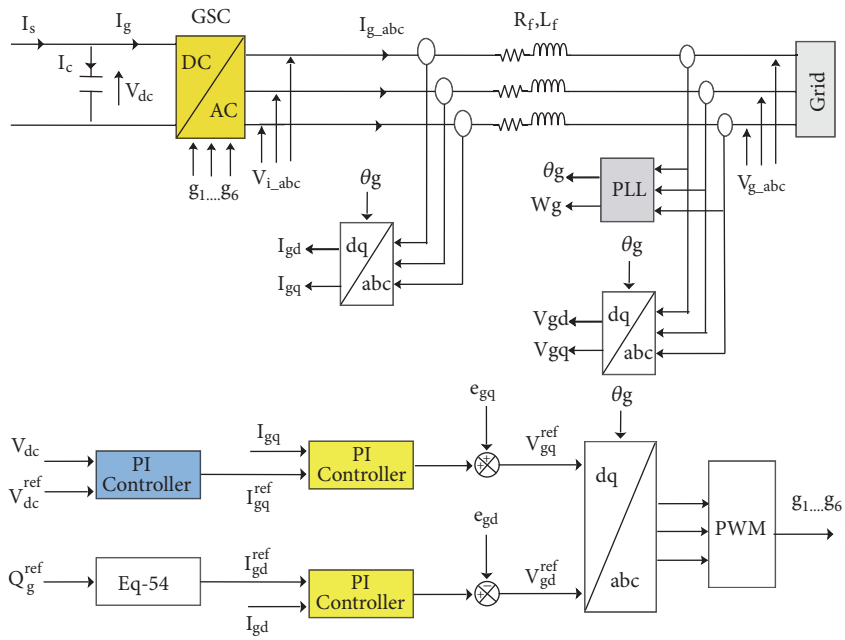

Figure 6: The Grid Side Converter Control by PI.

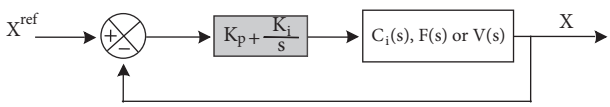

Figure 7: The Block diagram of the regulations.

the integral controller gain K_i), we use the compensation method for the closed loop system [6]; which is depicted in Figure 7.

$C_s(s)$, $F(s)$, $C_g(s)$, and $V(s)$ are the transfer functions of the stator currents, rotor filed, grid currents, and DC-Link Voltage, respectively, and are given by

$$C_s(s) = \frac{k_s}{1+\tau_s s};$$
$$F(s) = \frac{k_f}{1+\tau_f s};$$
$$C_g(s) = \frac{k_g}{1+\tau_g s};$$
$$V(s) = \frac{1}{Cs} \tag{57}$$

where $k_s = 1/R_s$, $\tau_s = \sigma L_s/R_s$; $k_f = M$, $\tau_f = L_r/R_r$ and $k_g = 1/R_f$, and $\tau_f = L_f/R_f$.

The PI controllers parameters (Proportional gain and Integral gain) of the stator side converter are given by

(i) For the stator currents

$$K_p^{i_s} = \frac{3\tau_s}{t_{rc}k_s};$$
$$K_i^{i_s} = \frac{3}{t_{rc}k_s} \tag{58}$$

(ii) For the rotor filed

$$K_p^{\Psi_r} = \frac{3\tau_f}{t_{rf}k_f};$$
$$K_i^{\Psi_r} = \frac{3}{t_{rf}k_f} \tag{59}$$

where t_{rf} and t_{rc} are the settling time for the rotor filed and the stator currents, respectively.

The PI controllers parameters of the grid side converter can be written:

(i) For the grid currents

$$K_p^{i_g} = \frac{3\tau_g}{t_{rg}k_g};$$
$$K_i^{i_g} = \frac{3}{t_{rg}k_g} \tag{60}$$

(ii) For the DC-Link Voltage

$$K_p^{v_{dc}} = 2\xi C\omega_0;$$
$$K_i^{v_{dc}} = C\omega_0^2;$$
$$\omega_0 = \frac{3}{t_{rv}\xi} \tag{61}$$

where t_{rg} and t_{rv} are the settling time for the grid currents and the DC-Link Voltage, respectively, and ξ is the damping coefficient generally taken 0.707.

We notice that it is necessary to design a controller for the outer loop (filed and voltage v_{dc}) with a slower response time than the dynamics of the inner loop (stator and grid currents).

5. Wind Energy Conversion (WEC) System Control by Linear-ADRC

This section focuses on the strategy adopted to control the WEC-System based a SCI-Generator by Linear-ADRC. The same control scheme presented in Figure 4 is used to control the stator side converter and the grid side converter while using the Linear-ADRC controller instead of the PI one. The general theory of the Linear-ADRC is detailed below.

5.1. Linear-ADRC Controller Design. The Active Disturbance Rejection Control (ADRC) is a robust control strategy, proposed by Han in 1995 [10]. The main advantage of this control is to compensate in real time the various external and internal disturbances. This control is based on the observer (ESO) which constitutes its kernel and which makes it possible to estimate the total disturbances. There are two types, the Linear-ADRC and NonLinear-ADRC. In order to reduce the model complexity and the controller computational, a Linear-ADRC design method is proposed and applied to control the SCI-Generator based WEC-System.

The observer used to estimate the process state variables and total distributions is represented by the model:

$$\begin{aligned} \dot{\hat{x}} &= A\hat{x} + Bu + L\left(y - \hat{y}\right) \\ \hat{y} &= C\hat{x} \end{aligned} \tag{62}$$

where $\hat{x} = [\hat{x}_1 \ \ \hat{x}_2]^T$ the estimated variables, $L = [\beta_1 \ \ \beta_2]^T$ is the observer gain vector, and A, B, C are gain matrices.

The extended state observer gains are determined by [10]

$$\begin{aligned} \beta_1 &= 2\omega_{obs}; \\ \beta_2 &= {\omega_{obs}}^2 \end{aligned} \tag{63}$$

ω_{obs} is determined according to the closed loop system poles to ensure both a fast dynamic of the observer and a minimum sensitivity to noise.

The canonical form of Linear-ARDC can be written:

$$\dot{y}(t) = f\left(y, d, u\right) + b_0 u(t) \tag{64}$$

where $f(y, d, u)$ represents the total (internal and external) disturbance, b_0 is known part of the process (system), $d(t)$ represents the external disturbance, and $u(t)$ and $y(t)$ are input and output of the process, respectively.

The combination of the linear ES-Observer and the corrector represents the Linear-ADRC whose structure is given in Figure 8.

In practice, we chose $k_p = \omega_c = 4/t_r$ with t_r being the system desired time. Also, we chose ω_{obs} in a range of $\omega_{obs} = 3 \sim 10\omega_c$ because the ES-Observer dynamic is faster than the system dynamic.

5.2. Stator Side Converter (SS-Converter) Control by Linear-ADRC. To control the stator side converter by ADRC, we elaborate three-Linear-ADRC controller; two Linear-ADRC controllers are used to regulate the stator currents i_{sd} and i_{sq} and the other one to control the direct rotor field Ψ_{rd} to track their reference. Figure 9 depicts the Active Disturbance Rejection Control of the stator side converter (SSC).

(i) The Stator Currents Controllers. The stator currents regulations are achieved by two Linear-ADRC controllers, where (40) and (41) are adapted to the canonical form of Linear-ARDC:

$$\dot{i}_{s_dq} = f_{s_dq}\left(y, d, u\right) + b_0^{i_{s_dq}} u_{s_dq} \tag{65}$$

For the d-axis stator current we have

$$\begin{aligned} f_{i_{sd}} &= -k_1 i_{sd} + \omega_s i_{sq} + k_2 \Psi_{rd} + \left(k_4 - b_0^{i_{sd}}\right) v_{sd} \\ b_0^{i_{sd}} &= k_4; \\ u_{i_{sd}} &= v_{sd} \end{aligned} \tag{66}$$

And for q-axis stator current we have

$$\begin{aligned} f_{i_{sq}} &= -k_1 i_{sq} - \omega_s i_{sd} - k_3 \Omega_{mec} \Psi_{rd} + \left(k_4 - b_0^{i_{sq}}\right) v_{sq} \\ b_0^{i_{sq}} &= k_4; \\ u_{i_{sq}} &= v_{sq} \end{aligned} \tag{67}$$

or $f_{i_{sd}}$ and $f_{i_{sq}}$ are the total (external and internal) disturbances affecting the stator currents i_{sd} and i_{sq}, respectively. $u_{i_{sd}}$ and $u_{i_{sq}}$ are the control inputs of the i_{sd} and i_{sq}, respectively. $b_0^{i_{sd}}$ and $b_0^{i_{sq}}$ are the known parts of the system parameters.

(ii) The Rotor Field Controller. We rewrite the field expression (42) under the canonical form (CF) of a Linear-ADRC regulator (65), and the expressions of the disturbance and the known part of the parameters are

$$\begin{aligned} f_{\Psi_{rd}} &= -k_6 \Psi_{rd} + \left(k_5 - b_0^{\Psi_{rd}}\right) i_{sd} \\ b_0^{\Psi_{rd}} &= k_5; \\ u_{\Psi_{rd}} &= i_{sd} \end{aligned} \tag{68}$$

where $f_{\Psi_{rd}}$ is the total (external and internal) disturbances affecting the field Ψ_{rd}. $u_{\Psi_{rd}}$ and $b_0^{\Psi_{rd}}$ are the control inputs and the known parts of the field Ψ_{rd}, respectively.

5.3. Grid Side Converter (GSC) Control by Linear-ADRC. Similarly to the stator side converter control, we elaborate three-Linear-ADRC controller; but in this case the two Linear-ADRC controllers are used to regulates the active and reactive power delivery into the grid by controls the grid currents i_{gd} and i_{gq} ((52) and (53)), and the other controller is used to maintain constant DC-Link Voltage.

(i) The Grid Currents Controllers. The grid currents regulations are achieved by two Linear-ADRC controllers, where the equations of i_{gd} and i_{gq} are adapted to the canonical form of Linear-ADRC.

$$\dot{i}_{g_dq} = f_{g_dq}\left(y, d, u\right) + b_0^{i_{g_dq}} u_{g_dq} \tag{69}$$

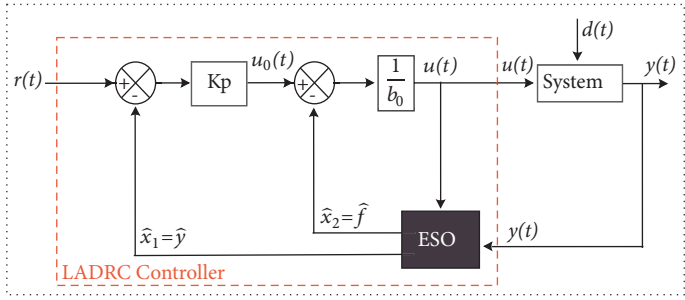

Figure 8: Linear-ADRC structure.

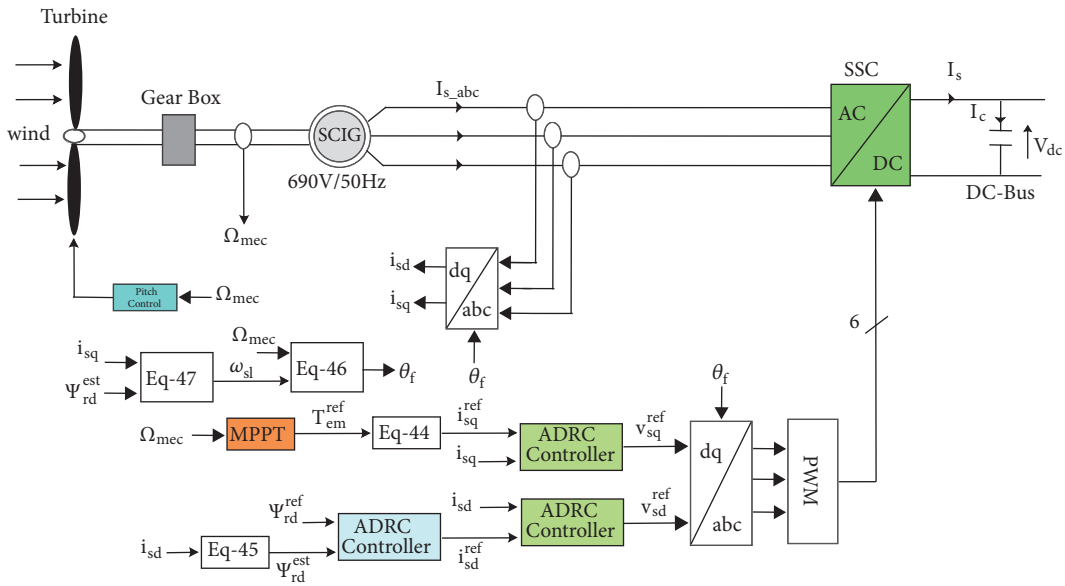

Figure 9: The Generator Side Converter Control by ADRC.

Substituting (52) and (53) into (69), we can write the grid currents equation as follows.

For direct axis current,

$$\begin{aligned} f_{i_{gd}} &= -k_7 i_{gd} + \omega_g i_{gq} + \left(k_8 - b_0^{i_{gd}}\right) v_{id} \\ b_0^{i_{gd}} &= k_8; \\ u_{i_{gd}} &= v_{id} \end{aligned} \tag{70}$$

And for quadrature axis current,

$$\begin{aligned} f_{i_{gq}} &= -k_7 i_{gq} + \omega_g i_{gd} - k_8 v_g + \left(k_8 - b_0^{i_{gq}}\right) v_{iq} \\ b_0^{i_{gq}} &= k_8; \\ u_{i_{gq}} &= v_{iq} \end{aligned} \tag{71}$$

(ii) The DC-Bus Voltage Regulation. The voltage expression of the DC-Link can be written as

$$C\frac{dv_{dc}}{dt} = i_s - i_g \tag{72}$$

If we neglect all the losses in converters, the powers P_s and P_g can be expressed as $P_s = i_s v_{dc}$ and $P_g = i_g v_{dc}$. Hence, to obtain the voltage equation for the DC-Link

$$C\frac{1}{2}\frac{dv_{dc}^2}{dt} = P_s - P_g \tag{73}$$

$$\frac{dv_{dc}^2}{dt} = \frac{2}{C}P_s - \frac{3}{C}v_{gq}i_{qg} \tag{74}$$

we put $W = {v_{dc}}^2$

$$\frac{dW}{dt} = k_9 P_s - k_{10} i_{qg} \tag{75}$$

with $k_9 = 2/C$ and $k_{10} = (3/C)v_g$.

The expressions of the disturbance $f_{v_{dc}}$ and the known part of the parameters $b_0^{v_{dc}}$ are

$$\begin{aligned} f_{v_{dc}} &= -k_9 P_s + \left(-k_{10} - b_0^{v_{dc}}\right) i_{gq} \\ b_0^{v_{dc}} &= -k_{10}; \\ u_{v_{dc}} &= i_{gq} \end{aligned} \tag{76}$$

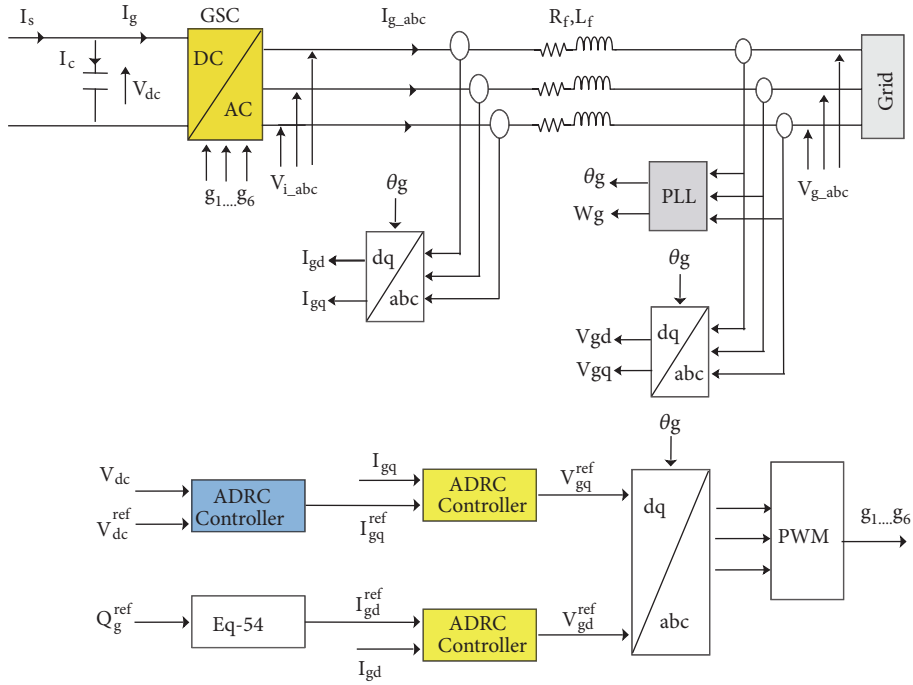

Figure 10: The Grid Side Converter Control by Linear-ADRC.

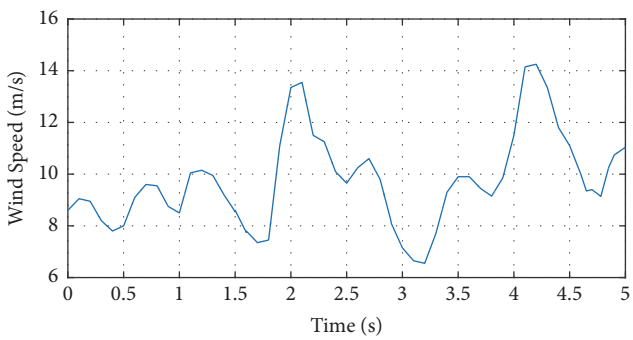

Figure 11: The Wind Speed Profile.

Figure 10 depicts the Active Disturbance Rejection Control of the grid side converter (GSC).

6. Simulation Results and Discussion

The simulations results of the presented control strategy are given and discussed in this section. The proposed WEC-System control has been simulated using the Matlab/Simulink. We have applied a variable wind speed profile as it is illustrated at Figure 11; the parameters of the WEC-System are given in the Appendix.

As it can be noticed in Figures 12 and 13, when the wind speed exceeds the rated speed, the mechanical speed of the turbine is limited by adjusting the pitch angle, and consequently the power coefficient and tip speed ratio of the turbine decrease.

Figures 14 and 15 present the simulation results of the stator side converter, for the two control strategies (ADRC control and PI control).

As it can be seen in Figures 14 and 15, the control by PI and the control by ADRC tracks their references, but the control by ADRC is faster (case of the electromagnetic torque and quadrature currents), more precise (case of the Rotor Field), and also without fluctuations (case of the direct current). In Figures 16–19 the simulation results of the grid side converter are presented.

As illustrated, the Linear-ADRC approach offers a faster trackness characteristic while controlling the DC-Link Voltage compared to the conventional approach by PI, where the DC-Link Voltage is maintained at its reference without presenting an overshoot at the transitional regime. Also, it can be noticed that the Linear-ADRC regulates the grid currents to their references.

The control of the active and reactive powers is also done. As can be seen in Figure 18, the power injected into the grid tracks its reference (the extracted power from the wind turbine minus joules and DC-Link losses). And the reactive power was set to zero to ensure a unit power factor. Hence the voltage and current of the grid are in phase as seen in Figure 19.

Finally, to test the robustness of the proposed control strategies, we have performed a change in the rotor resistance and the rotor inductance of the SCI-Generator by an increase of 50% and 10%, respectively, of their nominal value. The results obtained by LADRC controller and PI controller are highlighted in Figures 20 and 21.

Figures 20–22 show that the Linear-ADRC control responses presents better results than the control based on PI

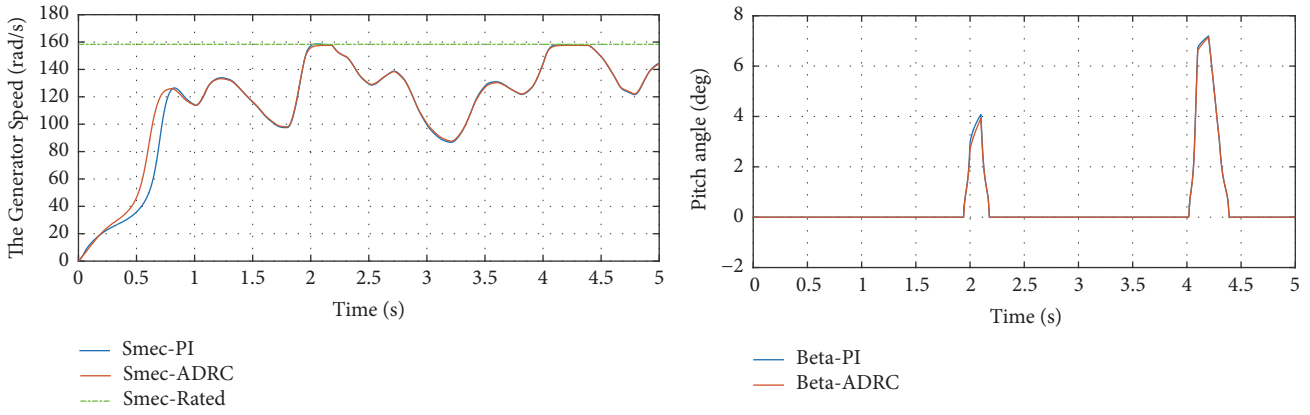

(a) Ω_{mec} (b) β

FIGURE 12: (a) The SCI-Generator Speed and (b) the blades pitch angel.

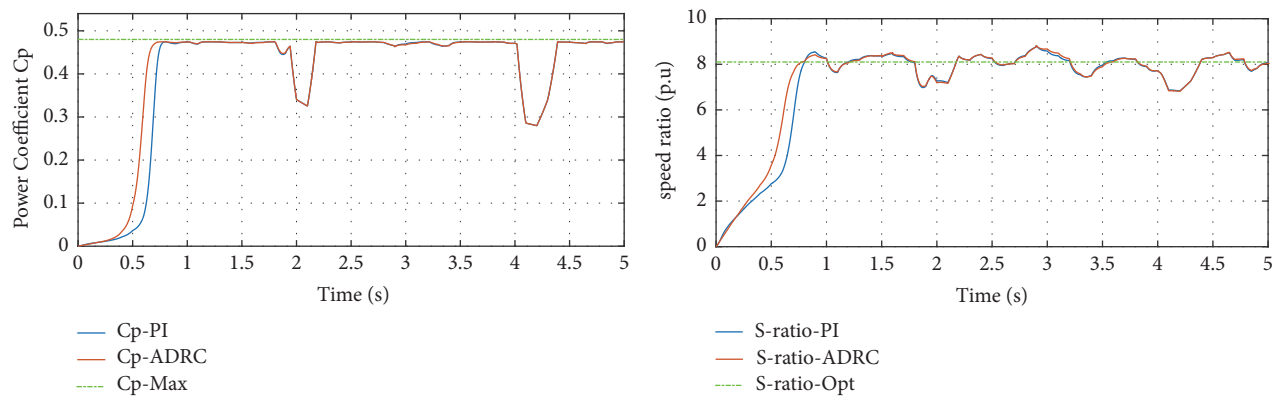

(a) C_p (b) λ

FIGURE 13: (a) The aerodynamic coefficient and (b) the turbine tip speed ratio.

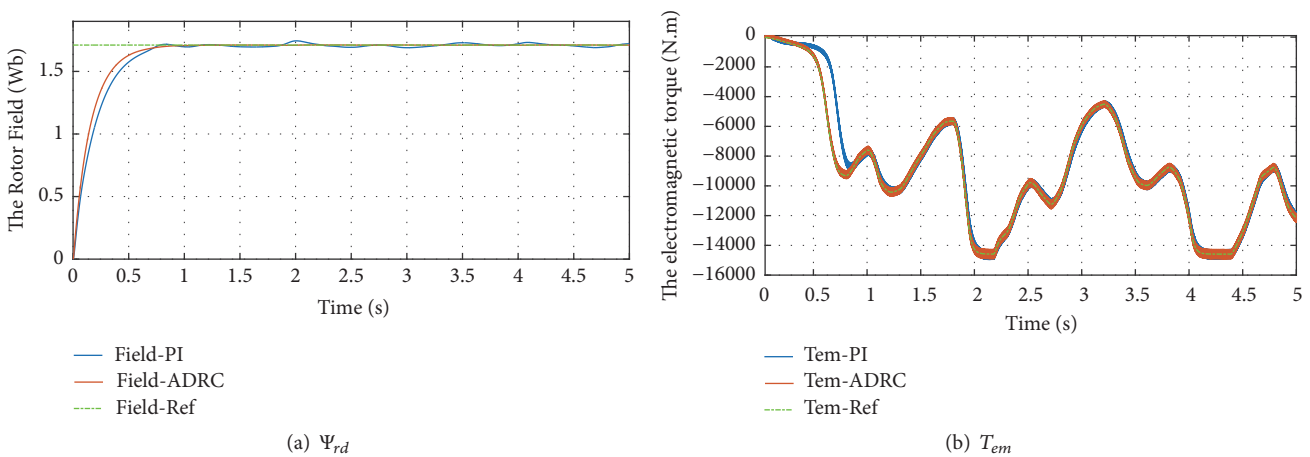

(a) Ψ_{rd} (b) T_{em}

FIGURE 14: (a) The direct rotor fluxes of the SCI-Generator and (b) the electromagnetic torque of the SCI-Generator.

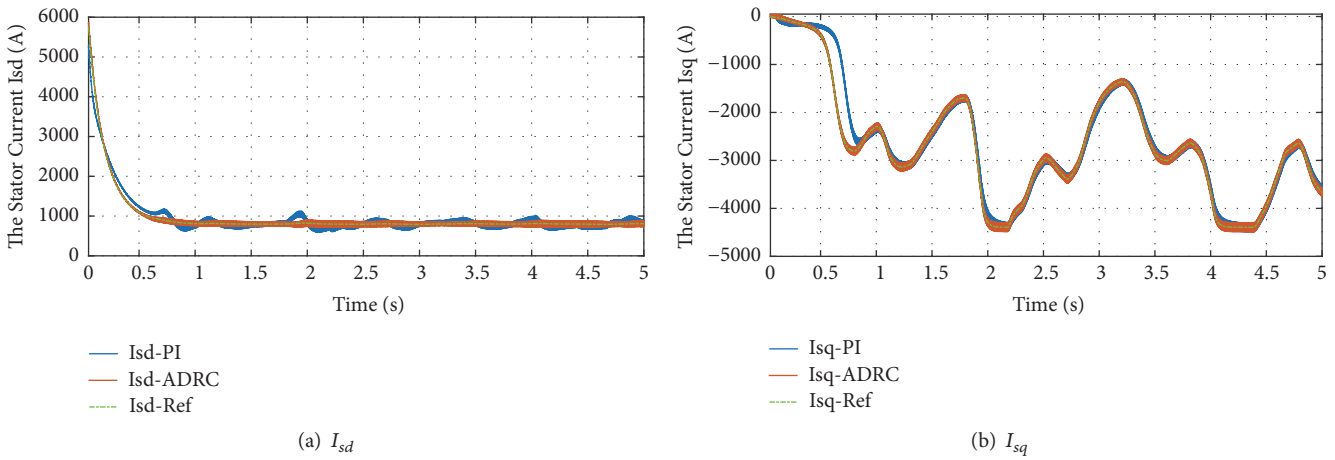

(a) I_{sd} (b) I_{sq}

FIGURE 15: The stator currents: (a) d-axis I_{sd} and (b) q-axis I_{sq}.

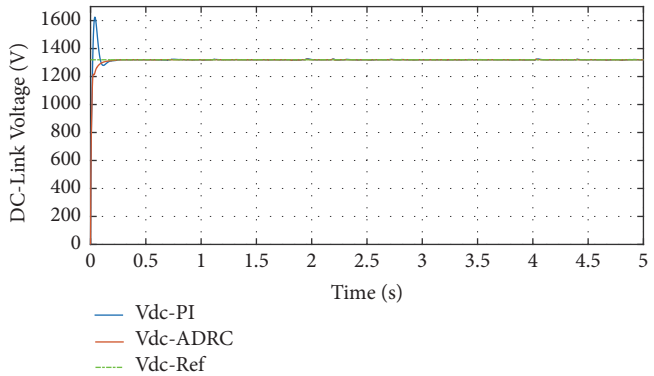

FIGURE 16: The DC-Link Voltage V_{dc}.

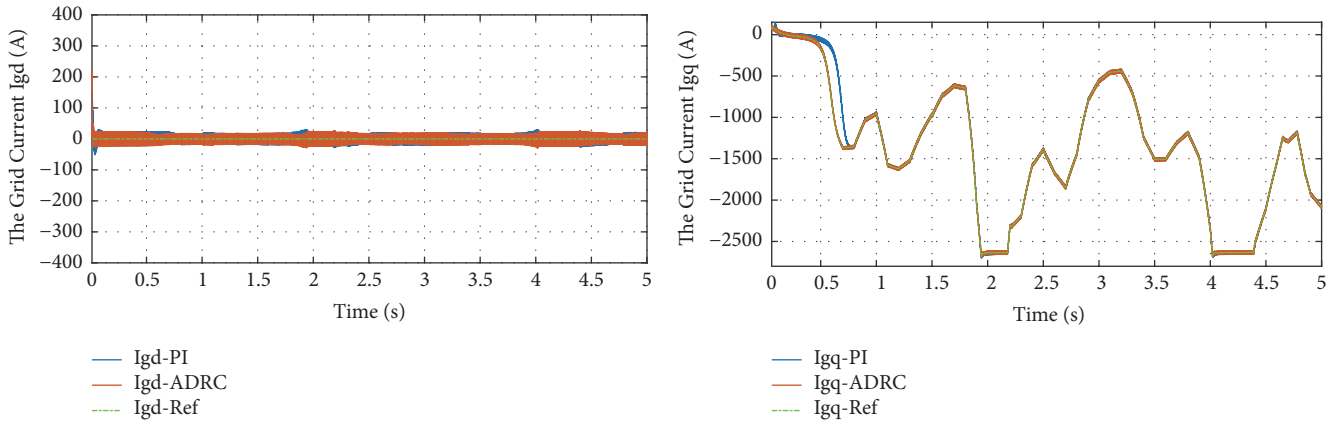

(a) I_{gd} (b) I_{gq}

FIGURE 17: The grid currents: (a) d-axis I_{gd} and (b) q-axis I_{gq}.

one. The Linear-ADRC is more robust and stable during the variation of the generator parameters.

The simulation results clearly indicate that the proposed Linear-ADRC strategy when applied to the WEC-System is able to track the desired values for both controls of the stator side converter and the grid side converter. Moreover, it is efficient in terms of stability and robustness regarding the variation of the generator parameters.

7. Conclusion

This paper deals with the modeling and control of a Wind Energy Conversion System using a Squirrel Cage Induction Generator. It seeks to evaluate the dynamical performances and sensitivity to SCI-Generator parameter changes with comparing the classical Indirect Field Oriented Control based on the PI controller and the new Linear Active Disturbance

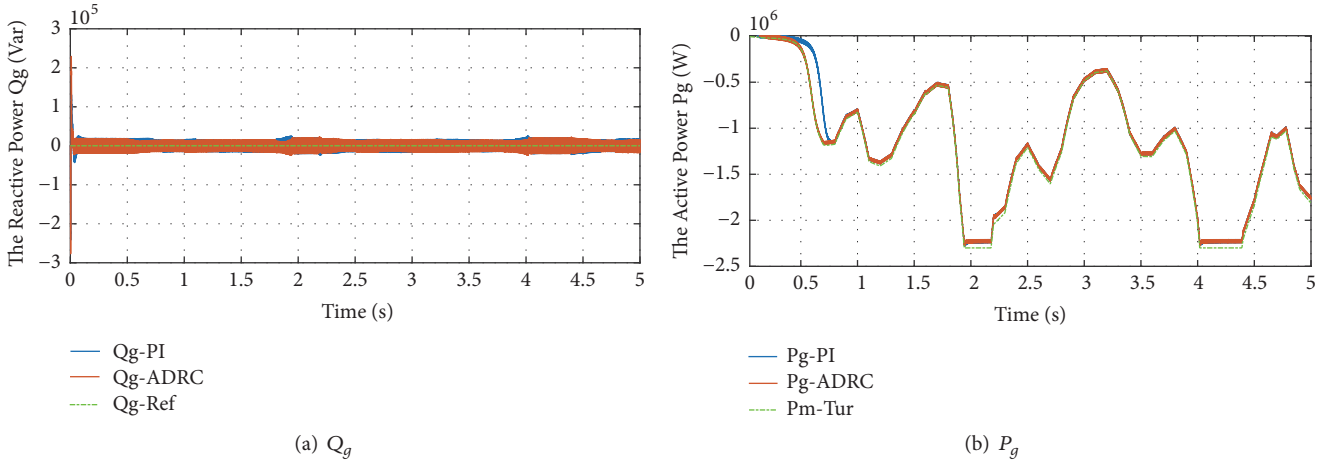

(a) Q_g (b) P_g

FIGURE 18: (a) The output reactive power Q_g of the grid and (b) the output active power P_g of the grid.

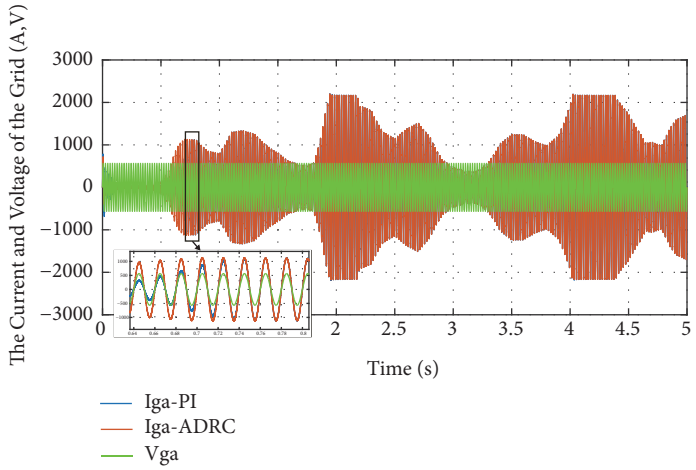

FIGURE 19: The grid voltage V_{ga} and the grid current I_{ga}.

Rejection Control. The Linear Active Disturbance Rejection controller and the PI controller are proposed to operate the wind turbine so as to extract the maximum power from the wind energy and to deliver it to utility power grid. It consists, on one hand, in controlling the stator currents in order to adapt the SCI-Generator rotational speed with the wind speed by acting on the generator electromagnetic torque (MPPT technique) and also control the rotor field and, on the other hand, in controlling through the grid currents, the active and reactive powers injected into the grid.

The simulation results show that the Linear-ADRC control strategy is efficient in terms of fast tracking and robustness to parameter sensitivity compared to the classical PI controller.

Appendix

The WEC-System parameters used for the simulation are given in the in the Table 1 for the turbine and Table 2 for the SCI-Generator and for the Grid side parameters in Table 3.

TABLE 1: The parameters of the turbine.

Parameters	Values
The rated power	2.3 MW
The rated wind speed	12 m/s
Density of Air	1.225 kg/m^3
Blade radius	38.72 m
The gearbox ratio G	63

Data Availability

There is no additional data to be included.

Disclosure

This work is an extended version of the author's conference paper that they have presented in the 6th International Renewable and Sustainable Energy Conference at Rabat,

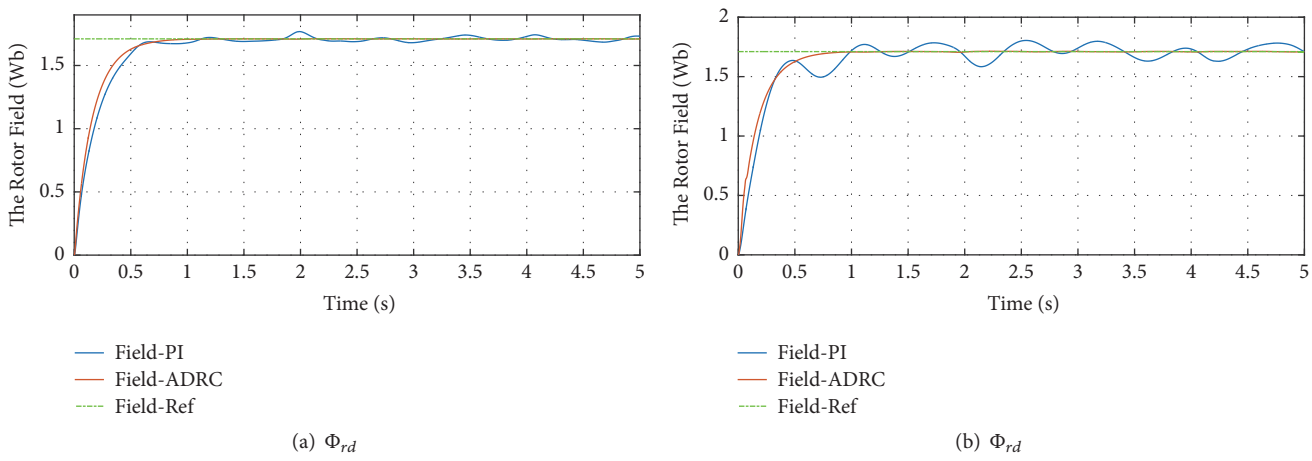

(a) Φ_{rd} (b) Φ_{rd}

Figure 20: (a) The direct rotor field for 50% R_r and (b) the direct rotor field for 10% L_r.

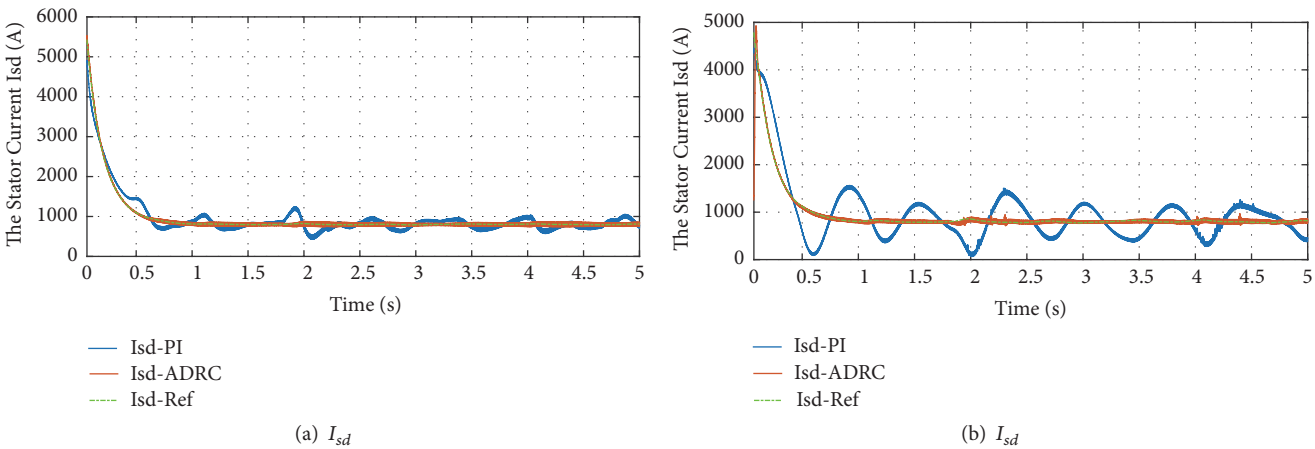

(a) I_{sd} (b) I_{sd}

Figure 21: (a) The direct stator current for 50% R_r and (b) the direct stator current for 10% L_r.

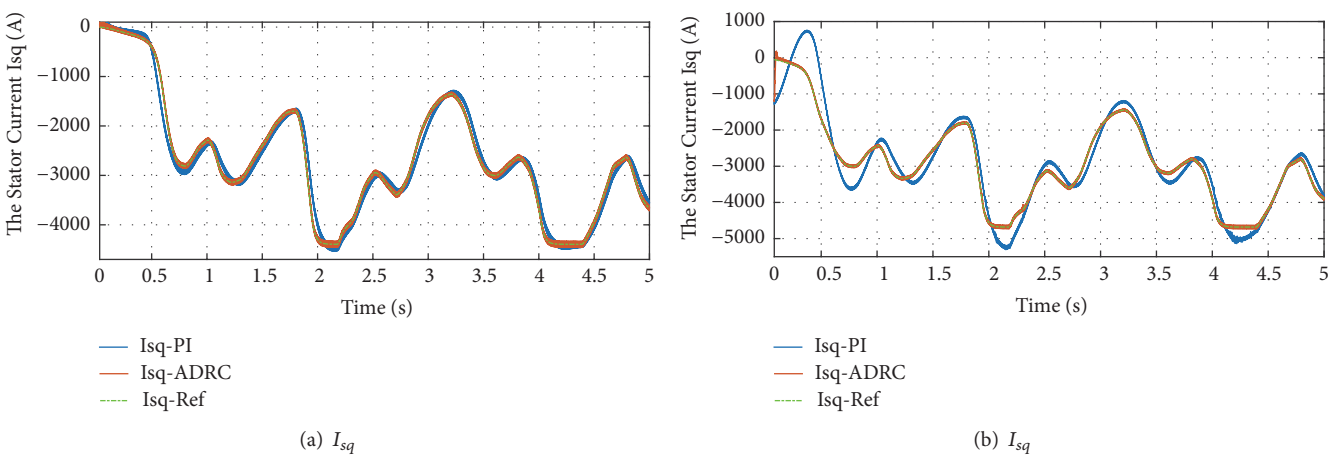

(a) I_{sq} (b) I_{sq}

Figure 22: (a) The quadrature stator current for 50% R_r and (b) the quadrature stator current for 10% L_r.

Table 2: The parameters of the SCI-Generator.

Parameters	Values
The Rated Power Pn	2.3 MW
The Rated Voltage Un	690 V
The Nominal Frequency	50 Hz
The Rated Rotor Speed	1512 tr/min
The Number of Pole Pairs	2
The Stator Resistance R_s	1.102 $m\Omega$
The Rotor Resistance R_r	1.497 $m\Omega$
The Stator Leakage Inductance L_{sl}	0.06492 mH
The Rotor Leakage Inductance L_{rl}	0.06492 mH
The Magnetizing Inductance M	2.13461 mH

Table 3: The parameters of the grid side.

Parameters	Values
The DC-Link Voltage V_{dc}	1320 V
The DC-Link Capacitor C	17316.17 μF
The Filter Resistance R_r	0.1838 Ω
The Filter Inductancer L_r	0.61187 mH

Morocco. This extended version explores the control of the grid side converter and the pitch angle control compared with the paper presented in the conference.

Conflicts of Interest

The authors declare that there are no conflicts of interest regarding the publication of this paper.

References

[1] S. Lalouni, D. Rekioua, K. Idjdarene, and A. Tounzi, "Maximum power point tracking based hybrid hill-climb search method applied to wind energy conversion system," *Electric Power Components and Systems*, vol. 43, no. 8-10, pp. 1028–1038, 2015.

[2] A. Meharrar, M. Tioursi, M. Hatti, and A. Boudghne Stambouli, "A variable speed wind generator maximum power tracking based on adaptative neuro-fuzzy inference system," *Expert Systems with Applications*, vol. 38, no. 6, pp. 7659–7664, 2011.

[3] M. Benchagra, M. Hilal, Y. Errami, M. Ouassaid, and M. Maaroufi, "Modeling and control of SCIG based variable-speed with power factor control," *International Review on Modelling and Simulations*, vol. 4, no. 3, pp. 1007–1014, 2011.

[4] M. Zribi, M. Alrifai, and M. Rayan, "Sliding mode control of a variable-speed wind energy conversion system using a squirrel cage induction generator," *Energies*, vol. 10, no. 5, article 604, 2017.

[5] M. G. Simões, B. K. Bose, and R. J. Spiegel, "Fuzzy logic based intelligent control of a variable speed cage machine wind generation system," *IEEE Transactions on Power Electronics*, vol. 12, no. 1, pp. 87–95, 1997.

[6] M. Benchagra, Y. Errami, M. Hilal, M. Maaroufi, M. Cherkaoui, and M. Ouassaid, "New control strategy for inductin generator-wind turbine connected grid," in *Proceedings of the 2012 International Conference on Multimedia Computing and Systems, ICMCS '12*, pp. 1043–1048, IEEE, 2012.

[7] K. A. Naik and C. P. Gupta, "Fuzzy logic based pitch angle controller/or SCIG based wind energy system," in *Proceedings of the Recent Developments in Control, Automation and Power Engineering, RDCAPE '17*, pp. 60–65, IEEE, October 2017.

[8] V. D. Dhareppagol and S. Nagendraprasad, "Modelling and simulation of wecs for maximum power extration and optimal efficincy control using squirrel cage induction generator," in *Proceedings of the Power, Communication and Information Technology Conference (PCITC '15)*, pp. 912–917, IEEE, October 2015.

[9] A. Edrisian, A. Goudarzi, I. E. Davidson, A. Ahmadi, and G. K. Venayagamoorthy, "Enhancing SCIG-based wind turbine generator performance through reactive power control," in *Proceedings of the Clemson University Power Systems Conference (PSC '15)*, IEEE, South Carolina, SC, USA, March 2015.

[10] R. Chakib, A. Essadki, and M. Cherkaoui, "Active disturbance rejection control for wind system based on a DFIG," *International Journal of Electrical Computer Energetic Electronic and Communication Engineering*, vol. 8, pp. 1306–1315, 2014.

[11] A. Boukhriss, A. Essadki, A. Bouallouch, and T. Nasser, "Maximization of generated power from wind energy conversion systems using a doubly fed induction generator with active disturbance rejection control," in *Proceedings of the 2nd World Conference on Complex Systems, WCCS 2014*, pp. 330–335, November 2014.

[12] A. Imad, S. El Hani, and A. Echchaachouai, "Robust active disturbance rejection control of a direct driven PMSG wind turbine," in *Proceedings of the International Renewable and Sustainable Energy Conference (IRSEC '17)*, pp. 1–6, IEEE, 2017.

[13] M. Arbaoui, A. Essadki, T. Nasser, and H. Chalawane, "Comparative analysis of ADRC & PI controllers used in wind turbine system driving a DFIG," *International Journal of Renewable Energy Research*, vol. 7, no. 4, pp. 1816–1824, 2017.

[14] M. A. H. Navas, J. L. A. Puma, and A. J. S. Filho, "Direct torque control for squirrel cage induction generator based on wind energy conversion system with battery energy storage system," in *Proceedings of the Power Electronics and Power Quality Applications (PEPQA '15)*, p. 16, IEEE, 2015.

[15] L. Liu, Z. Xu, and Q. Mei, "Induction motor drive system based on ADRC and PI regulator," in *Proceedings of the International Workshop on Intelligent Systems and Applications, ISA '09*, pp. 1–4, IEEE, May 2009.

[16] J. L. Domínguez-García, O. Gomis-Bellmunt, L. Trilla-Romero et al., "Vector control of squirrel cage induction generator for wind power," in *Proceedings of the 19th International Conference on Electrical Machines, ICEM '10*, pp. 1–6, IEEE, 2010.